

Temperature-Controlled Entangled-Photon Absorption Spectroscopy

Roberto de J. León-Montiel,^{1,*} Jiří Svozilík,^{2,3} Juan P. Torres,^{4,5} and Alfred B. U'Ren¹

¹*Instituto de Ciencias Nucleares, Universidad Nacional Autónoma de México,
Apartado Postal 70-543, 04510 Cd. Mx., México*

²*Yachay Tech, School of Physical Sciences & Nanotechnology, 100119, Urcuquí, Ecuador*

³*Joint Laboratory of Optics of Palacký University and Institute of Physics of CAS,
Faculty of Science, Palacký University, 17. listopadu 12, 771 46 Olomouc, Czech Republic*

⁴*ICFO - Institut de Ciències Fotoniques, Mediterranean Technology Park, 08860 Castelldefels (Barcelona), Spain*

⁵*Department of Signal Theory and Communications, Campus Nord D3,
Universitat Politècnica de Catalunya, 08034 Barcelona, Spain*

Entangled two-photon absorption spectroscopy (TPA) has been widely recognized as a powerful tool for revealing relevant information about the structure of complex molecular systems. However, to date, the experimental implementation of this technique has remained elusive, mainly because of two major difficulties. First, the need to perform multiple experiments with two-photon states bearing different temporal correlations, which translates in the necessity to have at the experimenter's disposal tens, if not hundreds, of sources of entangled photons. Second, the need to have *a priori* knowledge of the absorbing medium's lowest-lying intermediate energy level. In this work, we put forward a simple experimental scheme that successfully overcomes these two limitations. By making use of a temperature-controlled entangled-photon source, which allows the tuning of the central frequencies of the absorbed photons, we show that the TPA signal, measured as a function of the temperature of the nonlinear crystal that generates the paired photons, and a controllable delay between them, carries all information about the electronic level structure of the absorbing medium, which can be revealed by a simple Fourier transformation.

Nonlinear spectroscopy techniques have been used in analytical chemistry for extracting information about the dynamics and structure of complex systems, from small molecules to large light-harvesting photosynthetic complexes [1–5]. Even though in the optical regime these techniques are typically implemented using laser light, recent investigations suggest that the use of nonclassical states of light, such as entangled photon pairs, may open new and exciting avenues in experimental spectroscopy [6–33]. Remarkably, quantum light has enabled the observation of fascinating two-photon absorption (TPA) phenomena, such as the linear dependence of two-photon absorption rate on photon flux [6, 7], as well as the prediction of intriguing effects, such as inducing disallowed atomic transitions [8, 9], two-photon-induced transparency [10, 11], manipulation of quantum pathways of matter [12–17], and the control of entanglement in molecular processes [18, 19].

Among different quantum-enabled techniques, entangled-photon virtual-state spectroscopy [20–33] is a promising tool for extracting information about the intermediate, energy non-conserving electronic transitions [34, 35], that contribute to the two-photon excitation of a chemical or biological sample. In this technique, virtual-state transitions, a signature of the absorbing medium, are experimentally revealed by introducing a time delay between frequency-correlated photons and averaging over many experimental realizations with differing two-photon state characteristics [20].

Regardless of some experimental concerns already raised in the original virtual-state spectroscopy (VSS) proposal, VSS has been broadly considered as a new

promising route towards novel applications in ultra-sensitive detection [24, 36]. In this work, we propose an experimental scheme that overcomes the two major difficulties that one encounters when implementing the VSS technique, namely the need for averaging over experimental realizations differing in temporal correlations between the photons that are absorbed—which translates into the need for using hundreds of nonlinear crystals with different lengths—and the requirement of *a priori* knowledge of the absorbing medium's lowest-lying intermediate energy level.

Our scheme makes use of a temperature-controlled entangled-photon source to show that the TPA signal, to be recorded as a function of the temperature of the nonlinear crystal that produces the pair of absorbed photons, and an external signal-idler delay, yields information about the electronic level structure of the absorbing medium, which can be revealed by a simple Fourier transformation. Because of its simplicity, our proposed technique could be realized using standard and widely used temperature-controlled entangled-photon sources. In this way, our work opens up a new avenue towards the first experimental implementation of nonlinear quantum spectroscopy.

In order to describe our proposed spectroscopy technique (shown in Figure 1), let us consider first the interaction of a two-photon optical field $|\Psi\rangle$ with a medium described by a simple energy-level configuration where two-photon transitions occur from an initial state $|g\rangle$ to a doubly-excited final state $|f\rangle$ via non-resonant intermediate states denoted by $|j\rangle$. For simplicity, in the following, we will omit any other degree of freedom connected

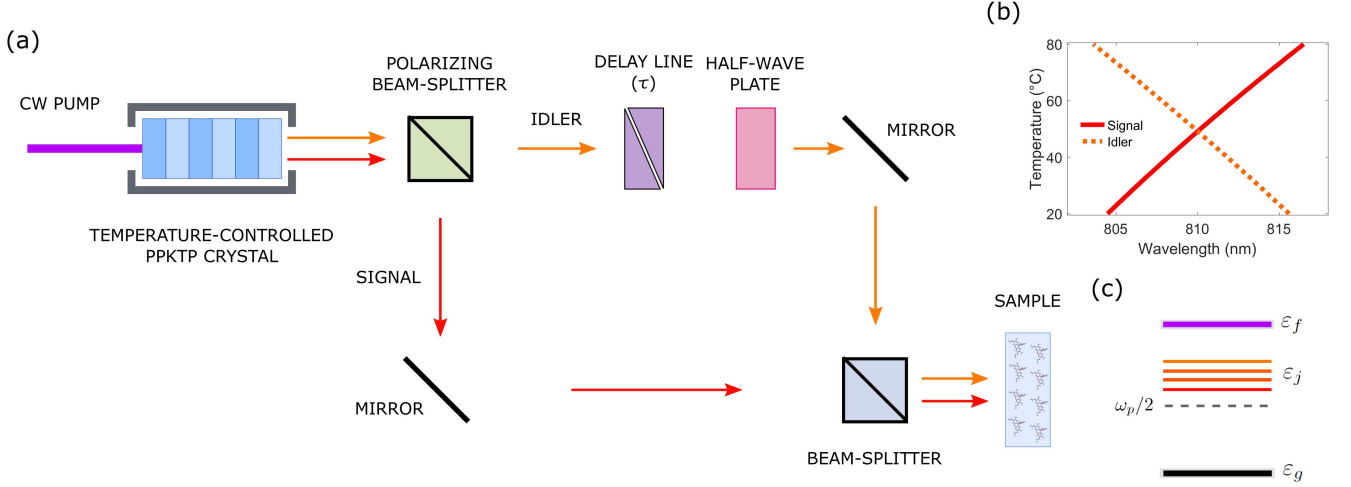


FIG. 1. Temperature-controlled quantum nonlinear spectroscopy. (a) Experimental scheme of the proposed technique. (b) Central wavelength of the down-converted photons as a function of the temperature of the PPKTP crystal, considering a continuous wave pump at 405 nm. (c) Model of the absorbing medium's electronic structure.

to vibrational modes of the sample, and assume that the lifetimes of intermediate states are much longer than the light-matter interaction time. Indeed, in this situation—which can be reached by selecting a proper correlation time between photons [20, 23], the effects due to dissipation in the single-excitation manifold (intermediate states) can be considered negligible.

The interaction of an electromagnetic field with a sample, in the dipole approximation, can be expressed as $\hat{H}(t) = \hat{d}(t) \hat{E}^{(+)}(t)$, where $\hat{d}(t)$ stands for the dipole-moment operator and $\hat{E}^{(+)}(t)$ for the positive-frequency part of the electric-field operator, which can be expressed as $\hat{E}^{(+)}(t) = \hat{E}_1^{(+)}(t) + \hat{E}_2^{(+)}(t)$. Each of the fields can then be written as

$$\hat{E}_{1,2}^{(+)}(t) = \int d\omega_{1,2} \sqrt{\frac{\hbar\omega_{1,2}}{4\pi\epsilon_0 c A}} \hat{a}_{1,2}(\omega_{1,2}) e^{-i\omega_{1,2}t}, \quad (1)$$

where c is the speed of light, ϵ_0 is the vacuum permittivity, A is the effective area of the field interacting with the sample, and $\hat{a}(\omega_{1,2})$ is the annihilation operator of a photonic mode characterized by a frequency $\omega_{1,2}$ bearing a specific spatial shape and polarization which, for the sake of simplicity, are not explicitly written.

By considering that the medium is initially in its ground state $|g\rangle$ (with energy ϵ_g), one can make use of second-order time-dependent perturbation theory to find that the probability that the medium is excited to the final state $|f\rangle$ (with energy ϵ_f), through a TPA process, is given by [22, 23]

$$P_{g \rightarrow f} = \left| \frac{1}{\hbar^2} \int_{-\infty}^{\infty} dt_2 \int_{-\infty}^{t_2} dt_1 M_{\hat{d}}(t_1, t_2) M_{\hat{E}}(t_1, t_2) \right|^2, \quad (2)$$

with

$$M_{\hat{d}}(t_1, t_2) = \sum_{j=1} D^{(j)} e^{-i(\epsilon_j - \epsilon_f)t_2} e^{-i(\epsilon_g - \epsilon_j)t_1}, \quad (3)$$

$$M_{\hat{E}}(t_1, t_2) = \langle \Psi_f | \hat{E}_2^+(t_2) \hat{E}_1^+(t_1) | \Psi \rangle + \langle \Psi_f | \hat{E}_1^+(t_2) \hat{E}_2^+(t_1) | \Psi \rangle, \quad (4)$$

where $D^{(j)} = \langle f | \hat{d} | j \rangle \langle j | \hat{d} | g \rangle$ are the transition matrix elements of the dipole-moment operator. Note from Eq. (3) that excitation of the medium proceeds through the intermediate states $|j\rangle$, with energy eigenvalues ϵ_j . Also, note that in Eq. (4), we have only written the terms in which one photon from each field contributes to the TPA process. In Eq. (4), $|\Psi_f\rangle$ denotes the final state of the optical field, which we take to be the vacuum state.

For the sake of simplicity and so as to show the technological readiness of our proposal, we consider a source of entangled two-photon states commonly found in many laboratories [see Figure 1(a)]. Collinear photon pairs with orthogonal polarizations are generated via type-II spontaneous parametric down-conversion (SPDC) in a periodically poled KTiOPO₄ (PPKTP) crystal of length L . We assume continuous wave pumping of the crystal at 405 nm. This configuration causes frequency anti-correlation of the down-converted photons and provides the strongest TPA signal (see supplementary materials and Refs. [23, 31, 32]). The wavelengths of the photons can be tuned around the degenerate wavelength (810 nm) changing the temperature T of the crystal [37]. The generated two-photon state can then be written as [38]

$$|\Psi\rangle = \left(\frac{T_e}{\sqrt{\pi}} \right)^{1/2} \int_{-\infty}^{\infty} \int_{-\infty}^{\infty} d\omega_s d\omega_i \delta(\omega_p - \omega_s - \omega_i) \times \text{sinc}\{T_e[\nu - \mu(T)]\} e^{i\omega_i \tau} \hat{a}_s^\dagger(\omega_s) \hat{a}_i^\dagger(\omega_i) |0\rangle, \quad (5)$$

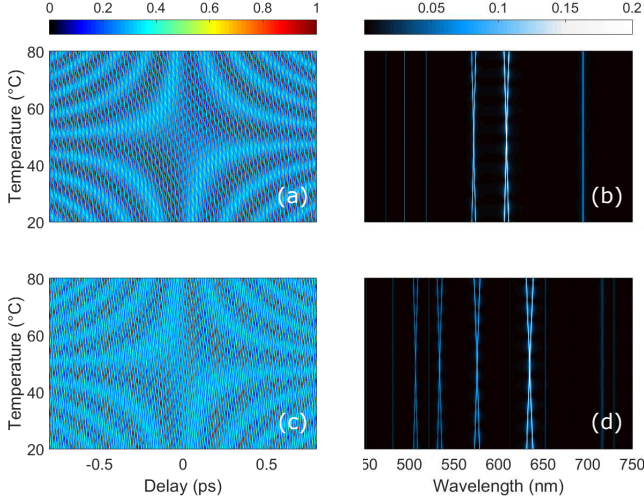


FIG. 2. Entangled-photon absorption spectroscopy for a system with two-photon transitions taking place via two [(a) and (b)] and four intermediate states [(c) and (d)]. (a) and (c): Normalized TPA signal as a function of the crystal temperature T and the external delay τ . (b) and (d): Normalized Fourier transform of the TPA signal with respect to the delay. We assume a source of entangled photon pairs with an entanglement time of $T_e = 0.87$ ps. For the absorbing medium, the energies of the levels (or wavelengths) are randomly chosen to be $\lambda_j^{(2)} \in \{563, 612\}$ nm, and $\lambda_j^{(4)} \in \{507, 534, 576, 635\}$ nm, respectively. Finally, in order to obtain the precise location of the intermediate states, the frequency axis is displaced by the degenerate frequency $\omega_0 = 2\pi c/(810\text{nm})$ [see supplementary materials for further details].

$$P_{g \rightarrow f}(\tau, T) = \frac{\left| \delta \left(\frac{\Delta_+}{2\pi} \right) \right|^2}{4\pi\hbar^2\epsilon_0^2 c^2 A^2} \frac{\omega_i^0(T) \omega_s^0(T)}{T_e} \left| \sum_{j=1} D^{(j)} \left\{ \frac{1 - e^{-i[\epsilon_j - \omega_i^0(T)](2T_e - \tau)}}{\epsilon_j - \omega_i^0(T)} + \frac{1 - e^{-i[\epsilon_j - \omega_s^0(T)](2T_e + \tau)}}{\epsilon_j - \omega_s^0(T)} \right\} \right|^2, \quad (6)$$

where $\Delta_+ = (\omega_p - \epsilon_f)/2$. For the sake of simplicity, we have displaced our energy levels so that $\epsilon_g = 0$. Furthermore, we have assumed the condition $\omega_s^0(T) + \omega_i^0(T) = \epsilon_f$, which guarantees that the two-photon field is resonant with the transition from the ground state $|g\rangle$ to the final state $|f\rangle$.

In order to show the usefulness of the technique proposed for revealing the electronic structure of a molecule, Figure 2 shows results for two examples. Figures 2(a) and (b) correspond to a system with two intermediate-state levels whose energies (in terms of wavelength) are randomly chosen to be $\lambda_j^{(2)} \in \{563, 612\}$ nm. Figures 2(c) and (d) correspond to another system with four intermediate-state levels arbitrarily chosen to be $\lambda_j^{(4)} \in \{507, 534, 576, 635\}$ nm. Figures 2(a) and (c) show the normalized TPA signals as a function of the crystal's temperature and the external delay between pho-

tons. The non-monotonic behavior of the TPA signal results from the interference between different pathways through which two-photon excitation of the medium occurs [20, 22] and, more importantly, it shows that the absorption properties of the sample can be tuned by properly controlling the time and frequency properties of the entangled photons [24].

where $\nu = \omega_i - \omega_s$, with ω_j ($j = p, s, i$) representing the frequencies of the pump, signal, and idler fields, respectively. The correlation (entanglement) time between the down-converted photons is given by $T_e = (N_s - N_i) L/4$, $N_{s,i}$ being the inverse group velocities of the signal and idler photons, respectively. In writing Eq. (5) we have assumed that an external delay τ between the generated photons has been introduced. As illustrated in Fig. 1(a), this can be experimentally implemented by introducing an optical delay line for one of the photons, once the pair has been split by means of a polarizing beam-splitter (PBS). Note that an additional half-wave plate is used in order to guarantee that both photons have the same polarization when impinging on the sample. The non-degeneracy of the photon wavelengths is given by the function $\mu(T) = \omega_i^0(T) - \omega_s^0(T)$, where $\omega_{i,s}^0(T)$ stands for the temperature-dependent central frequencies of each of the photon wavepackets. Figure 1(b) shows the dependence of the down-converted photon central wavelengths on the temperature of the PPKTP crystal.

The proposed quantum spectroscopy protocol works as follows. We consider the model system shown in Figure 1(c), in which the two-photon excitation energy of the medium $|g\rangle \rightarrow |f\rangle$ corresponds to the pump wavelength $\lambda_p = 405$ nm. By substituting Eqs. (3)-(5) into Eq. (2), one finds that the TPA signal is expressed as

tons. The non-monotonic behavior of the TPA signal results from the interference between different pathways through which two-photon excitation of the medium occurs [20, 22] and, more importantly, it shows that the absorption properties of the sample can be tuned by properly controlling the time and frequency properties of the entangled photons [24].

Figures 2(b) and (d) show the normalized Fourier transform of the TPA signals with respect to the external delay. Surprisingly, two characteristic patterns of X-shaped and straight lines appear. The X-shaped lines indicate the energy of intermediate states (ϵ_j), whereas the straight lines appear at the combined frequencies $\pm[\epsilon_j \pm \epsilon_k]$. The reason behind this contrasting behavior lies in the fact that the TPA signal of the former contain frequency components that are temperature dependent, while the latter are constant with temperature

(see calculations in the supplementary materials for a detailed analysis on the characteristics of the TPA signal’s Fourier transform).

Besides the remarkable advantage of not requiring many different sources of entangled photons in the implementation of two-photon absorption spectroscopy, our scheme permits the direct and straightforward extraction of the electronic structure of an arbitrary sample by simply identifying the X-shaped lines, without resorting to many-sample averaging or sophisticated data analysis. This is indeed a notable feature that previous proposals have failed to provide.

In conclusion, we have proposed an experimentally-feasible, novel scheme for absorption spectroscopy based on non-classical light. Previous proposals required the use of multiple nonlinear optics sources, which made its experimental implementation an unrealistic endeavor. Moreover, the acquisition of useful information from the measured data was not straightforward, calling for sophisticated data analysis in order to isolate information about the sought-after energy level structure of the sample under investigation. All of this has prevented the use and further development of entangled-photon virtual-state spectroscopy.

Contrary to all previous schemes, our proposal makes use of a *single* temperature-controlled nonlinear crystal, a state-of-the-art technology widely used nowadays. Furthermore, the information about the energy level structure can be obtained directly from the experimental data. This indeed constitutes a major simplification of the technique and establishes a new route towards its first experimental demonstration, a milestone in the development of a unique tool capable of providing new and detailed information about the dynamics and chemical structure of complex molecular systems.

ACKNOWLEDGMENTS

We acknowledge Jan Peřina Jr. for helpful discussions. We thank Javier A. López Alfaro for his help during the initial stage of the project, and Mario A. Quiroz-Juárez for his help in designing the schematic representation of the proposed technique. This work was supported by DGAPA-UNAM under the project UNAM-PAPIIT IA100718, and by CONACYT under the project CB-2016-01/284372. JS thanks the project No. 17-23005Y of Czech Science Foundation. JPT acknowledges financial support from Fundacio Cellex, from the Government of Spain through the Severo Ochoa Programme for Centres of Excellence in R&D (SEV-2015-0522), from Generalitat de Catalunya under the programs ICREA Academia and CERCA, and from the project 17FUN01 BeCOMe within the Programme EMPIR, and initiative co-founded by the European Union and the EMPIR Participating Countries. AU acknowledges support from PA-

PIIT (UNAM) grant IN104418, CONACYT Fronteras de la Ciencia grant 1667, and AFOSR grant FA9550-16-1-1458.

Supplementary material:

Temperature-Controlled Entangled-Photon Absorption Spectroscopy

In this supplementary material we present: (i) the explicit derivation of the different contributions arising from the Fourier transform of the two-photon absorption (TPA) signal that would be obtained in the experimental implementation of temperature-controlled entangled-photon absorption spectroscopy; and (ii) the relationship between the strength of the TPA signal and the spectral shape of the absorbed photons.

1. Temperature-controlled two-photon absorption

Let us start by writing the TPA probability as [23]

$$P_{g \rightarrow f} = \left| \frac{1}{\hbar^2} \int_{-\infty}^{\infty} dt_2 \int_{-\infty}^{t_2} dt_1 M_{\hat{d}}(t_1, t_2) M_{\hat{E}}(t_1, t_2) \right|^2, \quad (\text{S.1})$$

with

$$M_{\hat{d}}(t_1, t_2) = \sum_{j=1} D^{(j)} e^{-i(\varepsilon_j - \varepsilon_f)t_2} e^{-i(\varepsilon_g - \varepsilon_j)t_1}, \quad (\text{S.2})$$

$$M_{\hat{E}}(t_1, t_2) = \langle \Psi_f | \hat{E}_2^+(t_2) \hat{E}_1^+(t_1) | \Psi \rangle + \langle \Psi_f | \hat{E}_1^+(t_2) \hat{E}_2^+(t_1) | \Psi \rangle, \quad (\text{S.3})$$

where $D^{(j)} = \langle f | \hat{d} | j \rangle \langle j | \hat{d} | g \rangle$ are the transition matrix elements of the dipole-moment operator, and $\varepsilon_{g,j,f}$ are the energies of the ground, intermediate and final states, respectively. The states $|\Psi\rangle$ and $|\Psi_f\rangle$ are the initial and final states of the optical field. Note that, because we are interested in the absorption of two-photon states, the final state of the field is taken to be the vacuum. For the positive part of the electric field we write

$$\hat{E}_{1,2}^{(+)}(t) = \int d\omega_{1,2} \sqrt{\frac{\hbar\omega_{1,2}}{4\pi\varepsilon_0 c A}} \hat{a}_{1,2}(\omega_{1,2}) e^{-i\omega_{1,2}t}, \quad (\text{S.4})$$

where c is the speed of light, ε_0 is the vacuum permittivity, A is the effective area of the field interacting with the sample, and $\hat{a}(\omega_{1,2})$ is the annihilation operator of a photonic mode with frequency $\omega_{1,2}$.

Our model is then complete by defining the temperature-controlled entangled-photon state that interacts with the sample, as [38]

$$|\Psi\rangle = \left(\frac{T_e}{\sqrt{\pi}} \right)^{1/2} \int_{-\infty}^{\infty} \int_{-\infty}^{\infty} d\omega_s d\omega_i \delta(\omega_p - \omega_s - \omega_i) \text{sinc}\{T_e[\nu - \mu(T)]\} e^{i\omega_i \tau} \hat{a}_s^\dagger(\omega_s) \hat{a}_i^\dagger(\omega_i) |0\rangle, \quad (\text{S.5})$$

where $\nu = \omega_i - \omega_s$, with ω_j ($j = p, s, i$) representing the frequencies of the pump, signal, and idler fields, respectively. The correlation time between the down-converted photons is given by $T_e = (N_s - N_i)L/4$, $N_{s,i}$ being the inverse group velocities of the signal and idler photons, respectively. τ is an external delay between the generated photons, and their temperature-controlled non-degeneracy is given by the function $\mu(T) = \omega_i^0(T) - \omega_s^0(T)$, where $\omega_{i,s}^0(T)$ are the temperature-dependent central frequencies of the photons.

By substituting Eqs. (S.2)-(S.5) into Eq. (S.1), it is straightforward to find that the temperature-dependent TPA signal is given by

$$P_{g \rightarrow f} = \frac{\left| \delta \left(\frac{\Delta_+}{2\pi} \right) \right|^2}{4\pi\hbar^2\varepsilon_0^2 c^2 A^2} \frac{\omega_i^0(T) \omega_s^0(T)}{T_e} \left| \sum_{j=1} D^{(j)} \left\{ \frac{1 - e^{-i[\varepsilon_j - \omega_i^0(T)](2T_e - \tau)}}{\varepsilon_j - \omega_i^0(T)} + \frac{1 - e^{-i[\varepsilon_j - \omega_s^0(T)](2T_e + \tau)}}{\varepsilon_j - \omega_s^0(T)} \right\} \right|^2, \quad (\text{S.6})$$

where $\Delta_+ = (\omega_p - \varepsilon_f)/2$. For the sake of simplicity, we have displaced our energy levels, so that $\varepsilon_g = 0$. Furthermore, we have assumed the condition $\omega_s^0(T) + \omega_i^0(T) = \varepsilon_f$, which guarantees that the two-photon field is resonant with the two-photon induced atomic transition.

So as to understand the behavior of the Fourier transform of the TPA probability, in particular the “X” shape at the intermediate-level energy positions, we first realize that the photon spectral non-degeneracy as a function of the

crystal's temperature [depicted in Fig. 1(b) of the main manuscript] can be described by

$$\omega_s^0(T) = \omega_0 + \Delta(T), \quad (\text{S.7})$$

$$\omega_i^0(T) = \omega_0 - \Delta(T), \quad (\text{S.8})$$

where ω_0 is the degenerate frequency, $\omega_0 = 2\pi c/(810\text{nm})$ for our source, and $\Delta(T)$ is a temperature-dependent frequency shift.

By substituting Eqs. (S.7)-(S.8) into Eq. (S.6), one finds that the TPA signal can be written explicitly as

$$\begin{aligned} P_{g \rightarrow f} = \sum_{j,k=1} \bigg\{ & \left[\frac{1}{\varepsilon_j - \omega_0 - \Delta(T)} + \frac{1}{\varepsilon_j - \omega_0 + \Delta(T)} \right] \left[\frac{1}{\varepsilon_k - \omega_0 - \Delta(T)} + \frac{1}{\varepsilon_k - \omega_0 + \Delta(T)} \right] \\ & - \left[\frac{1}{\varepsilon_j - \omega_0 - \Delta(T)} + \frac{1}{\varepsilon_j - \omega_0 + \Delta(T)} \right] \left[\frac{e^{i[\varepsilon_k - \omega_0 - \Delta(T)](2T_e - \tau)}}{\varepsilon_k - \omega_0 - \Delta(T)} + \frac{e^{i[\varepsilon_k - \omega_0 + \Delta(T)](2T_e + \tau)}}{\varepsilon_k - \omega_0 + \Delta(T)} \right] \\ & - \left[\frac{e^{-i[\varepsilon_j - \omega_0 - \Delta(T)](2T_e - \tau)}}{\varepsilon_j - \omega_0 - \Delta(T)} + \frac{e^{-i[\varepsilon_j - \omega_0 + \Delta(T)](2T_e + \tau)}}{\varepsilon_j - \omega_0 + \Delta(T)} \right] \left[\frac{1}{\varepsilon_k - \omega_0 - \Delta(T)} + \frac{1}{\varepsilon_k - \omega_0 + \Delta(T)} \right] \\ & + \frac{e^{-i[\varepsilon_j - \varepsilon_k](2T_e - \tau)}}{[\varepsilon_j - \omega_0 - \Delta(T)][\varepsilon_k - \omega_0 - \Delta(T)]} + \frac{e^{-i[\varepsilon_j - \varepsilon_k](2T_e + \tau)}}{[\varepsilon_j - \omega_0 + \Delta(T)][\varepsilon_k - \omega_0 + \Delta(T)]} \\ & + \frac{e^{-i[\varepsilon_j - \varepsilon_k + 2\Delta(T)]2T_e} e^{-i(\varepsilon_j + \varepsilon_k - 2\omega_0)\tau}}{[\varepsilon_j - \omega_0 + \Delta(T)][\varepsilon_j - \omega_0 - \Delta(T)]} + \frac{e^{-i[\varepsilon_j - \varepsilon_k - 2\Delta(T)]2T_e} e^{i(\varepsilon_j + \varepsilon_k - 2\omega_0)\tau}}{[\varepsilon_j - \omega_0 - \Delta(T)][\varepsilon_j - \omega_0 + \Delta(T)]} \bigg\}. \end{aligned} \quad (\text{S.9})$$

We are now ready to discuss the signals appearing in the Fourier transform of the TPA signal. Firstly, we realize that the terms that contribute to the Fourier transform of Eq. (S.9) are only those depending on the delay τ . Therefore, the first line represents a constant contribution centered at zero frequency; the second and third lines produce a signal centered at the frequencies $\pm[\tilde{\varepsilon}_j \pm \Delta(T)]$, with $\tilde{\varepsilon}_j = \varepsilon_j - \omega_0$. Note that when the photons are degenerate, i.e. $\Delta(T) = 0$, the signals appear at the position of the intermediate-state energy values. Remarkably, as the temperature is increased (or reduced), the signal splits into two new ones separated by an energy gap equal to $2\Delta(T)$, thus producing a frequency plot similar to the one shown in Fig. 1(b) of the main text. This is the reason for the “X” shape of the signals centered at the intermediate-state energies. Finally, the fourth and fifth lines produce signals centered at the frequencies $\pm[\varepsilon_j \pm \varepsilon_k]$, which are independent of the temperature. These contributions are the straight, constant lines that accompany the intermediate-state X-shaped signals.

2. Role of photon spectra in two-photon absorption spectroscopy

In the main text we highlight the fact that the TPA signal shows its maximum amplitude when the absorbed photons are frequency anti-correlated. Although this has been extensively discussed in Refs. [23, 31, 32], it is worth describing the reason behind this important result.

In order to obtain a general form of the TPA signal, we assume that the nonlinear crystal is now pumped by a Gaussian pulse with temporal duration T_p . In this situation, the two-photon state can be written as [23]

$$\begin{aligned} |\Psi\rangle = & \left(\frac{T_p T_e}{2\pi\sqrt{\pi}} \right)^{1/2} \int_{-\infty}^{\infty} \int_{-\infty}^{\infty} d\omega_s d\omega_i \exp \left[-T_p^2 (\omega_p - \omega_s - \omega_i)^2 \right] \text{sinc} \{ T_e [\nu - \mu(T)] \} \\ & \times e^{i\omega_i \tau} \hat{a}_s^\dagger(\omega_s) \hat{a}_i^\dagger(\omega_i) |0\rangle. \end{aligned} \quad (\text{S.10})$$

The frequency correlations of the down-converted photons can be tuned by carefully selecting the values of T_p and T_e . Figures 3(a)-(c) show the joint probability distribution of the two-photon state, i.e.

$$S(\omega_s, \omega_i) = \frac{T_p T_e}{2\pi\sqrt{\pi}} \exp \left[-2T_p^2 (\omega_p - \omega_s - \omega_i)^2 \right] \text{sinc}^2 \{ T_e [\nu - \mu(T)] \}, \quad (\text{S.11})$$

which represents the probability of detecting a signal photon, with frequency ω_s , in coincidence with an idler photon, of frequency ω_i . Frequency anti-correlated photons [Fig. 3(a)] are obtained when $T_p \gg T_e$, whereas for $T_p \ll T_e$ we obtain frequency-correlated photons [Fig. 3(c)]. In the particular case when $T_p = T_e/2$, frequency quasi-uncorrelated pairs of photons [Fig. 3(b)] are generated.

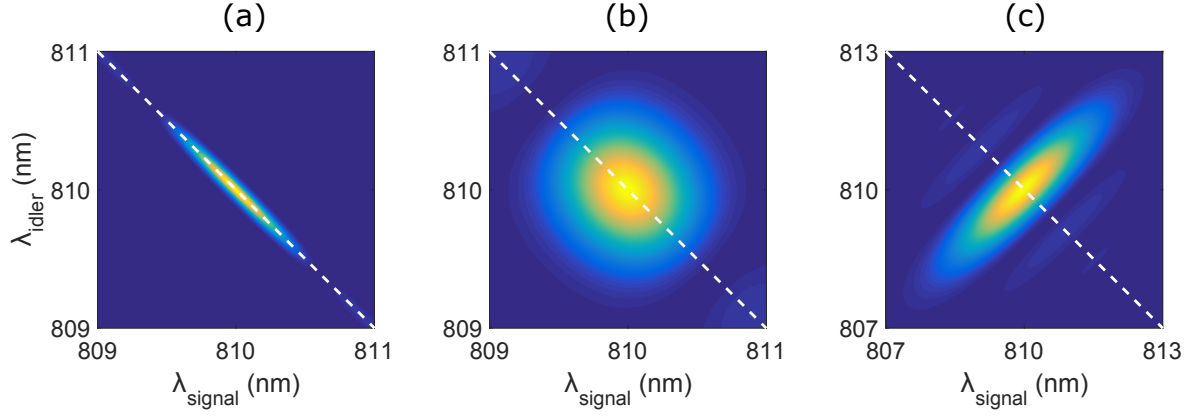


FIG. 3. Joint spectrum of the two-photon state for different values of T_p : (a) $T_p = 4$ ps, (b) $T_p = 435$ fs, and (c) $T_p = 100$ fs. In all cases, the entanglement time is set to $T_e = 0.87$ ps. The dashed line represents the final-state two-photon resonance condition. Note that the largest overlap between the two-photon fields and the final state transition occurs for frequency anti-correlated photons.

By making use of Eq. (S.10), it is straightforward to find that the corresponding TPA signal is given by

$$P_{g \rightarrow f} = \frac{T_p}{T_e} \frac{\sqrt{2\pi} \omega_i^0(T) \omega_s^0(T)}{\hbar^2 \varepsilon_0^2 c^2 A^2} \exp[-2T_p^2 (\omega_p - \omega_s - \omega_i)] \times \left| \sum_{j=1} D^{(j)} \left\{ \frac{1 - e^{-i[\varepsilon_j - \omega_i^0(T)](2T_e - \tau)}}{\varepsilon_j - \omega_i^0(T)} + \frac{1 - e^{-i[\varepsilon_j - \omega_s^0(T)](2T_e + \tau)}}{\varepsilon_j - \omega_s^0(T)} \right\} \right|^2. \quad (\text{S.12})$$

Note that the strength of the TPA signal is essentially controlled by the ratio T_p/T_e , which maximizes when $T_p \gg T_e$, i.e., when the photons are frequency anti-correlated. Physically, this important result can be understood in terms of the overlap between the joint spectrum of the entangled photons and the two-photon resonance condition (represented by the dashed line in Fig. 3). We can observe that the TPA signal is enhanced by increasing the overlap between the joint spectrum and the dashed line. Therefore, as one might expect, the maximum overlap is obtained for a continuous wave pump, with its frequency coinciding exactly with the two-photon resonance condition.

* roberto.leon@nucleares.unam.mx

- [1] R. R. Ernst, G. Bodenhausen, and A. Wokaun, *Principles of nuclear magnetic resonance in one and two dimensions* (Clarendon Press, Oxford, 1987).
- [2] S. Mukamel, *Principles of Nonlinear Optical Spectroscopy* (Oxford University Press, New York, 1995).
- [3] P. Hamm and M. Zanni, *Concepts and methods of 2D infrared spectroscopy* (Cambridge University Press, New York, 2011).
- [4] M. Cho, *Two-dimensional optical spectroscopy* (CRC Press, Boca Raton, 2009).
- [5] J. Yuen-Zhou, J. J. Krich, I. Kassal, A. S. Johnson, and A. Aspuru-Guzik, *Ultrafast Spectroscopy: Quantum Information and Wavepackets* (IOP Publishing, Bristol, 2014).
- [6] J. Javanainen and P. L. Gould, Phys. Rev. A **41**, 5088 (1990).
- [7] D.-I. Lee and T. Goodson III, J. Phys. Chem. B **110**, 25582 (2006).
- [8] A. Muthukrishnan, G. S. Agarwal, and M. O. Scully, Phys. Rev. Lett. **93**, 093002 (2004).
- [9] M. Scully, *International Conference on Quantum Information*, OSA Technical Digest (CD) (Optical Society of America, 2011), paper QMA1.
- [10] H.-B. Fei *et al.*, Phys. Rev. Lett. **78**, 1679 (1997).
- [11] A. R. Guzmán *et al.*, J. Am. Chem. Soc. **132**, 7840 (2010).
- [12] O. Roslyak and S. Mukamel, Phys. Rev. A **79**, 063409 (2009).
- [13] O. Roslyak, C. A. Marx, and Shaul Mukamel, Phys. Rev. A **79**, 033832 (2009).
- [14] M. G. Raymer, A. H. Marcus, J. R. Widom, and D. L. P. Vitullo, J. Phys. Chem. B **117**, 15559 (2013).
- [15] F. Schlawin, K. E. Dorfman, B. P. Fingerhut, and S. Mukamel, Nat. Commun. **4**, 1782 (2013).
- [16] F. Schlawin, K. E. Dorfman, and S. Mukamel, Phys. Rev. A **93**, 023807 (2016).
- [17] F. Schlawin and A. Buchleitner, New J. Phys. **19**, 013009 (2017).
- [18] M. Shapiro and P. Brumer, Phys. Rev. Lett. **106**, 150501 (2011).
- [19] M. Shapiro and P. Brumer, *Quantum control of molecular processes* (Wiley-VCH, Weinheim, 2012).

- [20] B. E. A. Saleh, B. M. Jost, H.-B. Fei, and M. C. Teich, Phys. Rev. Lett. **80**, 3483 (1998).
- [21] J. Kojima and Q.-V. Nguyen, Chem. Phys. Lett. **396**, 323 (2004).
- [22] J. Perina, B. E. A. Saleh, and M. C. Teich, Phys. Rev. A **57**, 3972 (1998).
- [23] R. de J. León-Montiel, J. Svozilik, L. J. Salazar-Serrano, and J. P. Torres, New J. Phys. **15**, 053023 (2013).
- [24] K. E. Dorfman, F. Schlawin, and S. Mukamel, Rev. Mod. Phys. **88**, 045008 (2016).
- [25] F. Schlawin, J. Phys. B **50**, 203001 (2017).
- [26] H. Oka, Phys. Rev. A **81**, 063819 (2010).
- [27] J. P. Villabona-Monsalve, O. Calderón-Losada, M. Nuñez Portela, and A. Valencia, J. Phys. Chem. A **121**, 7869 (2017).
- [28] O. Varnavski, B. Pinsky, and T. Goodson III, J. Phys. Chem. Lett. **8**, 388 (2017).
- [29] H. Oka, Phys. Rev. A **97**, 063859 (2018).
- [30] H. Oka, Phys. Rev. A **97**, 033814 (2018).
- [31] J. Svozilik, J. Perina Jr., and R. de J. León-Montiel, J. Opt. Soc. Am. B **35**, 460 (2018).
- [32] J. Svozilik, J. Perina Jr., and R. de J. León-Montiel, Chemical Physics **510**, 54 (2018).
- [33] R. K. Burdick, O. Varnavski, A. Molina, L. Upton, P. Zimmerman, and T. Goodson III, J. Phys. Chem. A **122**, 8198 (2018).
- [34] B. W. Shore, Am. J. Phys. **47**, 262 (1979).
- [35] J. J. Sakurai, Modern Quantum Mechanics (Addison-Wesley, New York, 1994).
- [36] F. Schlawin, K. E. Dorfman, and S. Mukamel, Acc. Chem. Res. **51**, 2207 (2018).
- [37] A. Fedrizzi, T. Herbst, A. Poppe, T. Jennewein, and A. Zeilinger, Opt. Express **15**, 15377 (2007).
- [38] A. Fedrizzi, T. Herbst, M. Aspelmeyer, M. Barbieri, T. Jennewein, and A. Zeilinger, New J. Phys. **11**, 103052 (2009).